Bagheri et al., J Nucl Med Radiat Ther 2018 9:6
DOI: 10.4172/2155-9619.1000390

Journal of
Nuclear Medicine & Radiation Therapy

Research Article Open Access

Dendrimer Nanoparticles Conjugated ^{99m}TC as a Promising Bioimaging Probe

Hamed Bagheri[1], Fatemeh Vosough T[2] and Habibollah Dadgar[3]*

[1]*Radiation and Wave Research Center, AJA University of Medical Science, Tehran, Iran*
[2]*Departments of Physics, University of Zanjan, Zanjan, Iran*
[3]*RAZAVI Cancer Research Center, RAZAVI Hospital, Imam Reza International University, Mashhad, Iran*

Abstract

Recent progress in nanoscale tumor targeting may able to deliver radionuclides for improving the outcome of both cancer diagnosis and therapy. Dendrimers are large and complex molecules with well-defined nanoscale structure. Current overview highlights the dendritic nano-probes for Single Photon Emission Computed Tomography (SPECT) because of low sensitivity and specificity. Conjugating radiopharmaceuticals and dendrimers has produced bioimaging probes which have prolonged enhanced stability, reduced toxicity and improved target specificity. However, the application of dendrimers to nuclear medicine is still new technique for improving images. Overall, the multidisciplinary structure of dendrimers makes them good choices for medical imaging or treatment.

Keywords: PAMAM dendrimer; Micro-SPECT imaging; ^{99m}TC radiopharmaceuticals

Introduction

Nuclear medicine agents

In the field of Nuclear Medicine procedures, radio-pharmaceuticals are administered to the patients and their radiations are detected by sensors. In fact, radiopharmaceuticals are consisting of two components, a carrier and a tracer amount of a radionuclide regarding defined radiation types [1]. Routinely, scintigraphy imaging detects the emission of the tracer in a planar form, whereas in Single Photon Emission Tomography (SPECT), the gamma camera detects and reconstructs the tracer emissions as 3D images [2]. Innovative modalities such as Positron Emission Tomography (PET) uses compounds labeled with positron-emitting radionuclides to provide functional images. PET is based on the detection of two photons produced when the positron is emitted from the nucleus of an unstable radionuclide and annihilates with its antiparticle (an electron). PET scanner has higher sensitivity and specificity than SPECT and is able to detect picomolar concentrations of a tracer. PET and SPECT combined with CT scans can compensate the attenuation and provide corrections for emission images with a more accurate anatomic correlation of tracer uptake in the body [3-5]. Moreover, low signal-to-noise ratios (SNR) may make it sophisticated to distinguish targets from the background. The growth of nanotechnology has brought challenging diagnosis and therapy innovations in medicine particularly in the Nuclear Medicine imaging. Consequently, dendrimers in the field of nuclear medicine have concentrated on improving the primary diagnosis of tumors and on their treatment. Conjugating nano-drugs to water-soluble, nontoxic, biocompatible polymers is well established [6-8] which includes long blood circulation time, decreased toxicity [9-13]. Meanwhile, dendrimers are a new class of highly branched spherical polymers that are highly soluble in aqueous solution and have a unique surface of many functional groups. Compared with many other types of dendrimers, Polyamidoamine (PAMAM) dendrimers with huge amine groups have the advantage of conjugating with other molecules *via* an amide linkage [14,15]. As a challenge in Nuclear Medicine, both SPECT and PET are limited by a low spatial resolution. The main aim of the current review is an assessment of the dendrimers effects on SPECT for improving quality of images. Furthermore, we focused on a wide range of applications of linker molecules for increasing SNR correlated with images.

Molecular imaging modalities

SPECT and PET are two major molecular imaging systems which are used in nuclear medicine. Both techniques use radio-labeled molecules to verification of molecular processes that can be visualized, quantified and tracked over time. The impact of molecular imaging has been on a greater understanding of characterization of disease and detection, and evaluation of treatment [16-18]. SPECT is the most established modality and standard imaging procedures have been widely available. The radiotracers used in SPECT emit gamma rays, as opposed to PET isotopes which are positron emitters like ^{18}F(T1/2=110 min). The SPECT radiotracers have relatively long half-lives from a few hours to a few days (^{99m}Tc T1/2=6.0 h; ^{111}In T1/2=67.3 h; ^{123}I T1/2=13.3 h; ^{201}Tl T1/2=72.9 h). As well as an improvement the imaging agents [19,20], focusing on the development of new SPECT imaging systems with increased sensitivity and improve image quality and resolution is a hot topic recently [21].

Image quality

Image quality in Nuclear Medicine, especially in SPECT, is determined by attenuation, scatter, spatial and energy resolution, image noise and contrast. Moreover, numerous studies have demonstrated the integration of CT with SPECT for attenuation correction that improved the image quality, and the CT also provides fair anatomical images [22]. The CT image is obtained prior to the SPECT image and assesses an attenuation map of the spatial distribution of the

***Corresponding author:** Habibollah Dadgar, RAZAVI Cancer Research Center, RAZAVI Hospital, Imam Reza International University, Mashhad, Iran; E-mail: reza.lt.dadgar@gmail.com

Received October 08, 2018; **Accepted** November 23, 2018; **Published** November 30, 2018

Citation: Bagheri H, Vosough FT, Dadgar H (2018) Dendrimer Nanoparticles Conjugated 99mTC as a Promising Bioimaging Probe. J Nucl Med Radiat Ther 9: 390. doi: 10.4172/2155-9619.1000390

attenuation coefficients. In one hand, patient movement between the two acquisitions can lead to wrong attenuation correction and misregistration. Scatter in SPECT images can reduce image contrast, so various scatter correction algorithms have been reviewed previously [23]. On the other hand, although these algorithms maybe improve image qualities these days nanoparticles application offer a modern technology for this issue. Image quality depends on resolution, sensitivity, a field of view and detector area [24].

Cardiology PET *vs.* SPECT

The spatial resolution of SPECT is approximately 10 mm while for PET is 5 mm. As a comparison between PET and SPECT studies, despite the challenges of spatial resolution in SPECT, it is shown that SPECT can be a good choice in various clinical applications, especially in cardiology. SPECT is well done in myocardial perfusion imaging. While the guidelines also suggested the use of [^{18}F] FDG PET to assess myocardial viability. Most common ^{99m}TC radiotracers used in cardiovascular imaging shown in Figure 1.

Oncology PET *vs.* SPECT

PET with multiple radiotracers being used for imaging ([^{18}F] FDG for glucose metabolism, [^{18}F] FLT for cell proliferation, ^{18}F labeled RGD for angiogenesis, [^{18}F] ethylcholine forprostate, etc.). However, SPECT is used for bone scintigraphy. In a study on the use of [^{18}F] FDG PET *vs*. SPECT (using ^{99m}Tc-HMDP) in detecting bone metastases from breast cancer [25] showed that sensitivity and accuracy of SPECT were more than PET (85%) *vs* (17%) and (96%) *vs*. (85%) respectively.

Neurology PET *vs.* SPECT

^{99m}Tc-hexamethylpropyleneamineoxime (^{99m}Tc-HMPAO) SPECT and [^{18}F] FDGPET is used to detect cerebral perfusion and metabolic abnormalities in Alzheimer's disease [26]. In neurology, ^{123}I is preferred for improved blood-brain barrier penetration as compared to the larger ^{99m}Tc SPECT imaging. Common SPECT radiotracers used in neurology was shown in Table 1.

Technetium-99m labeling

Research on ^{99m}Tc radiopharmaceuticals commenced after the development of the ^{99}Mo/^{99m}Tc generators [27]. The availability of short-lived (half-life: 6h) is a major factor for use of this radioisotope. ^{99m}Tc derivatives are used in several diagnostic procedures, from the use of pertechnetate for thyroid uptake to the use of ^{99m}Tc-octreotide derivatives for imaging neuroendocrine tumors. A major advantage of ^{99m}Tc for radiopharmaceutical development is a varietal chemistry in which making it a good choice to produce many complexes with specific desired characteristics. There are hundreds of ^{99m}Tc complexes useful for diagnostic procedures, of which over thirty are used in clinical studies. ^{99m}Tc radiopharmaceuticals can be categorized as first, second or third generation products, depending on their level of complexity.

First generation

This generation was employed by taking advantage of the easy absorption, distribution and excretion properties of the ^{99m}Tc. Previous studies led to the thyroid (^{99m}TcO4$^-$), liver (^{99m}Tc-colloids), bone (^{99m}Tc-phosphonates) and kidney (^{99m}Tc-DTPA) [28].

Figure 1: Most common ^{99m}TC labeling for cardiovascular imaging.

	Ammonia core	EDA core	
Generation	molecular mass/ number of terminal groups	molecular mass	number of terminal groups
0	359/3	516	4
1	1043/ 6	1428	8
2	2411/12	3252	16
3	5147/24	6900	32
4	10619/48	14196	64
5	21563/96	28788	128
6	43451/192	57972	256
7	87227/384	116340	512
8	174779/768	233076	1024
9	349883/1536	466548	2048
10	700091/3072	933492	4096

Table 1: Theoretical properties of PAMAM dendrimers.

Second generation

Nuclear magnetic resonance (NMR) spectroscopy, mass spectroscopy (MS) and X-ray diffraction persuade researchers to verify the structure and biological behavior of the ^{99m}Tc agents and also conjugating other tracers to the ^{99m}Tc. Consequently, precise design of legends led to the discovery of imaging agents for perfusion in the myocardium and brain. The widely used cardiac imaging agents ^{99m}Tc-MIBI (sestamibi, Cardiolite), ^{99m}Tc-tetrofosmin, and the brain imaging agents ^{99m}Tc-HMPAO (exametazime, Ceretec) and ^{99m}Tc-ECD (bicisate, Neurolite) are the result of the above strategy in the development of ^{99m}Tc complexes [29-31].

Third generation

Development these agents led to the labeling the bifunctional chelating agent (BFCA) and new chemistries such as the Tc-tricarbonyl, Tc-nitrido, Tc-HYNIC. ^{99m}Tc-HYNICEDDA- TOC, developed as an alternative to 111In-octreotide, and ^{99m}Tc-TRODAT-1 are the best examples of third generation ^{99m}Tc radiopharmaceuticals [32,33].

Dendrimers

Dendrimers are nano-sized with a homogeneous and monodisperse structure which is an ideal candidate as targeting nano-objects regarding the vectorization of diagnostic or therapeutic agents through the complexation of very diverse metallic ions [34]. These days, however, the dendrimers are interesting particles for nuclear medicine imaging with attracting a considerable interest to develop novel approaches in cancer imaging, molecular diagnosis.

PAMAM dendrimers

Tomalia et al. synthesized the first generation of Polyamidoamine (PAMAM) dendrimers [35] which have ethylene-diamine (EDA) core and an amidoamine repeat branching structure (Figure 2).They are synthesized *via* Michael addition of amino groups of EDA with methyl acrylate, followed by admiration of the resulting esters with EDA, and generation 0 is formed (Figure 3). A repetition of these two synthetic steps adds another layer of branching units and produces next generation. The size of dendrimer grows linearly in diameter as a function of added generations, approximately 1 nm per generation (Tables 1 and 2). Each new generation also doubles the number of terminal groups and approximately doubles the molecular weight of the previous generation. Figure 3 shows the synthesis of amine (NH_2) terminated PAMAM dendrimers that are cationic; however, there are also neutral hydroxyls (OH) and anionic carboxyl (COOH) terminated PAMAM dendrimers. Due to half completion of the monomer addition, the carboxyl terminated dendrimers are called half generations. Regarding to this issue, dendrimers can covalently attach several drug molecules, targeting groups. For avoiding sterical snag and to provide drug with a reactive group for diagnostic and therapy, a variety of spacer molecules can be linked to the drug and as such used for conjugation reaction with dendrimers. The presence of hydrophilic terminal groups makes dendrimers highly water soluble. The solubility increases with the generation number; the higher generation, the higher number of terminal groups, leads to increased surface charge and polarity. So as will discuss fellow, G2 to G5 dendrimer generations is used for suffering more drug or radiopharmaceuticals in the region of interests for imaging. Physicochemical characteristics of amine-terminated PAMAM dendrimers are shown in Table 1 as well.

Discussion

Regarding the promising dendrimer structure and their valuable properties, numerous researches have offered to design ^{99m}Tc-labeled dendrimers for diagnostic applications in nuclear medicine. Moreover, the Starburst structure of dendrimers allows multivalent attachment of chelators and targeting moieties.Pioneering work has been carried out by Mukhtar et al [36]. They reported two water-soluble generation (G), G1 and G2 dendrimers, with porphyrin cores possessing terminal iminodiacetic acid groups as chelating moieties for the successful

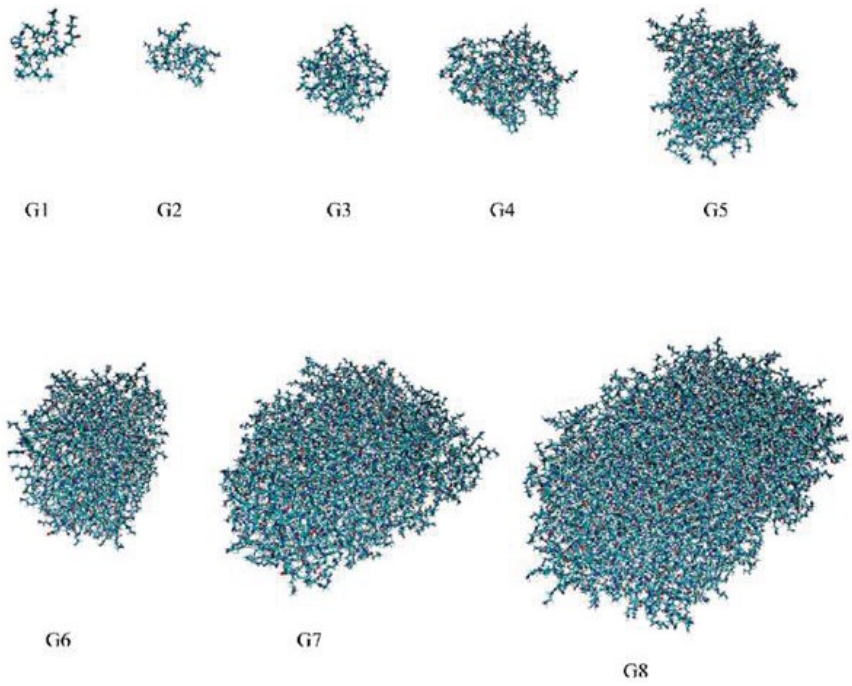

Figure 2: Schematic structure of G1 to G8 dendrimers.

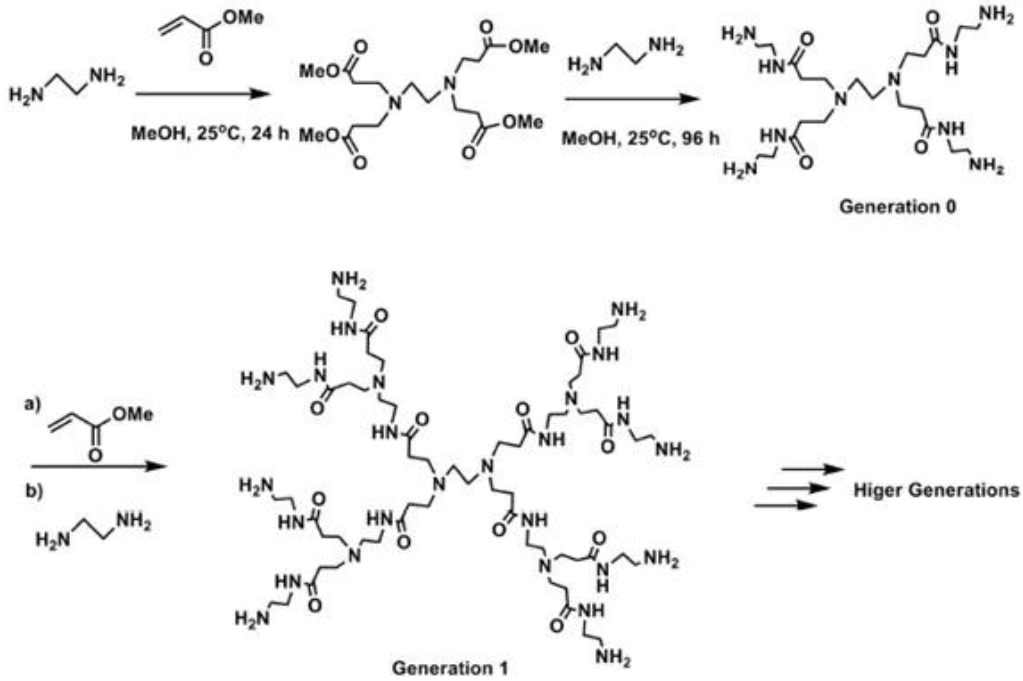

Figure 3: Alteration of G0 generation of dendrimers to G1.

Diameter (nm)	Molecular weight	Number of surface groups	Generation
1.5	517	4	0
2.2	1430	8	1
2.9	3256	16	2
3.6	6909	32	3
4.5	14215	64	4
5.4	28826	128	5
6.7	58048	256	6
8.1	116493	512	7
9.7	467162	1024	8
11.4	934720	2048	9

Table 2: Physiochemical characteristics of amine terminated PAMAM dendrimers.

radiolabeling (95%) with ^{99m}Tc. Another study was performed by Agashe et al. [37] using this technique to investigate the biodistribution in mice of G5 (polypropylene imine) dendrimers (PPI) coated with mannose (M-PPI) or lactose (L-PPI) so as to explore the potential of these systems as drug carriers. They demonstrated that ^{99m}Tc-labeled carbohydrate coated dendrimers are cleared from the systemic circulation faster than uncoated dendrimers. Conventional nuclear medicine imaging has low specificity and sensitivity using radiolabeled tumor specific agents. Multiple-step amplification pre-targeting greatly increases the accumulation of radioactivity in the target tissue. One approach to prepare a well-defined of ^{99m}Tc-labeled dendrimer for SPECT imaging is to incorporate a single high-affinity ^{99m}Tc ligand at the focal point of high-generation dendrons [38]. Other trials carried out by Shen et al. [39] by involving the G5 PAMAM dendrimers functionalized at the primary amines periphery with DTPA as a ^{99m}Tc-ligand and folic acid (FA) as a targeting agent for folate receptors over-expressed in cancer cells [40]. Their synthesized radiolabeled PAMAM–FA [conjugate 1] had excellent *in vitro/in vivo* stability, and the biodistribution analysis in tumor-bearing nude mice indicated its rapid blood clearance and preferential accumulation at the tumor site within 6 hours, which was further confirmed by micro-SPECT imaging (Figure 4).

A subsequent study [41] by the same group demonstrated, both through biodistribution and micro-SPECT imaging studies, that indirect FA conjugation with G5 PAMAM through a PEG spacer increased the tumor uptake: PEG is hydrophilic and structurally flexible, potentially evading the recognition and phagocytosis by macrophage cells in the lymphatic system. This enables folic acid modified with PEG to selectively bind with a metastatic tumor-cell leading to receptor-mediated endocytosis. Such a study confirmed the potential of an FA-conjugated dendrimer as a promising imaging tool for cancer diagnosis (Figure 5).

Further Applications of Dendrimers

Many authors with increasing the solubility and decrease the non-specific cellular uptake suggest the primary amine on the surface of PAMAM dendrimer were partially converted to acetamide moieties in the presence of acetic anhydride and triethylamine [42]. Folic acid (FA) is an optimal targeting ligand for selective delivery of attached imaging and therapeutic agents which has high affinity to the folate receptor [43,44] even after labeling with therapeutic/diagnostic agents and it was used for targeting of FR-positive tumors. The limited distribution

of its receptor (FR) in normal tissues and over-expressed in cancer cells made folic acid relatively satisfactory targeting ligand [45]. Recent studies have demonstrated that the conjugation dendrimers with fluorescein may lead to a preferential distribution of the cargo in the targeted tumor cells [46-54]. Emiting fluorescence from dendrimers cannot yet be adapted for clinical use; however, exogenous fluorophores can be conjugated to the exteriorprimary amine groups to enable detection by the respective imaging modalities. Generation size changes the pharmacokinetic and pharmaco-dynamic properties of dendrimers and increasing the size alter their permeability across the vascular wall, excretion route, and their recognition and uptake by the reticulo-endothelial system. Therefore, smaller sized dendrimers may be used for renal imaging, whereas larger sized preferentially used for imaging the liver and spleen.

Conjugation of FA to the partially acetylated dendrimers was carried out *via* condensation between the c-carboxyl group of FA and the primary amine of the dendrimer. Zhang et al. have confirmed that synthesized ^{99m}Tc radio-labeled dendrimer PAMAM-G5-folic acid conjugate showed certain accumulation in KB tumor-bearing nude mice [55]. Their Micro-SPECT imaging further confirmed the conjugate of ^{99m}Tc-G5-Ac-FA-1B4M DTPA concentrated in the tumor as time increased and had excellent *in vitro/in vivo* stability and rapid clearance from blood (Figure 6).

Numerous *in vivo* studies have demonstrated that 80% of the ^{99m}Tc-G5-Ac-FA-DTPA and ^{99m}Tc-G5-Ac-DTPA remained intact within 6h in the blood of normal mice [39,55]. Moreover, their biodistribution was investigated with KB tumor–bearing nude mice. For this assessment, the mice were maintained on a folate-deficient diet for the duration of the experiment to minimize the circulating levels of FA. As a result, ^{99m}Tc-G5-Ac-DTPA and ^{99m}Tc-G5-Ac-FA-DTPA fast cleared from the blood, decreasing from 11.75% injected dose/gram (ID/g) at 2 h to 5.60% ID/g at 6 h for ^{99m}Tc-G5-Ac-DTPA and from 12.59% ID/g at 2 h to 4.00% ID/g at 6 h for ^{99m}Tc-G5-Ac-FA-DTPA. Both agents remained at a low level up to 6 h in the FR-negative organs, including the brain. Micro-SPECT imaging also confirmed the uptake of ^{99m}Tc-G5-Ac-FA-DTPA in the FR-positive tumors, liver, and kidneys [39,55]. Investigating on ^{99m}Tc-G5-Ac-pegFA-DTPA, ^{99m}Tc-G5-Ac-FA-DTPA and ^{99m}Tc-G5-Ac DTPA showed that PEGylation of the PAMAM dendrimer-FA conjugate improves the tumor targeting and may be used as a targeted delivery system for imaging labels and therapeutic drugs [41,55].

Parrott et al. have recently developed dendrimers based on aliphatic polyester dendrons labeled with ^{99m}Tc for dynamic SPECT imaging using rats. It was reported that SPECT images correlated well with data obtained from biodistribution studies. Furthermore, synthesized dendrimers were rapidly cleared from the bloodstream and were nontoxic [56]. Avidin is a quickly internalizing molecule into either normal hepatocytes or cancer cells, especially ovarian and colorectal adenocarcinoma cells, which expresses b-D-galactose receptors [57-61] and extremely easy to conjugate with biotin.

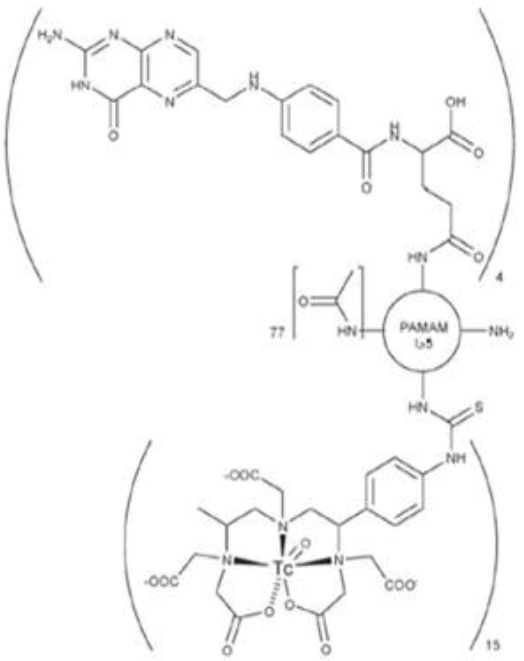

Conjugate 1

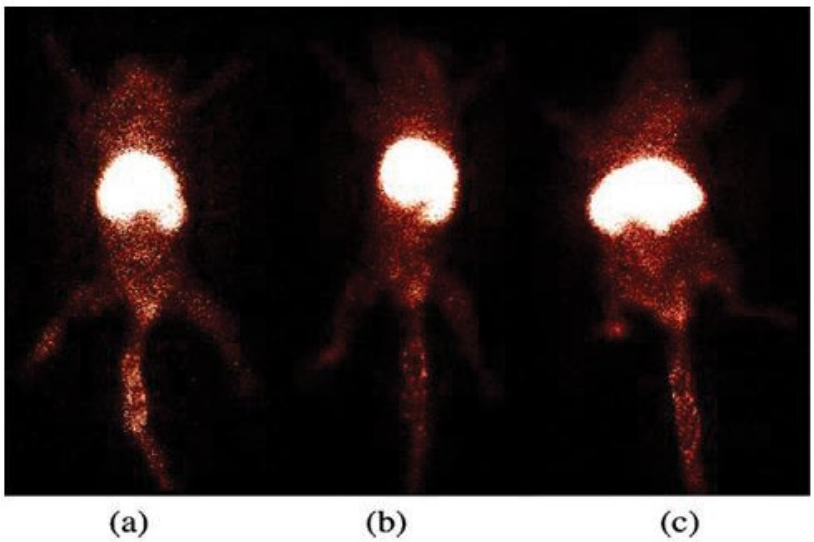

Figure 4: Micro-SPECT imaging of normal healthy mouse at 2, 4 and 6 h after injection the tracer.

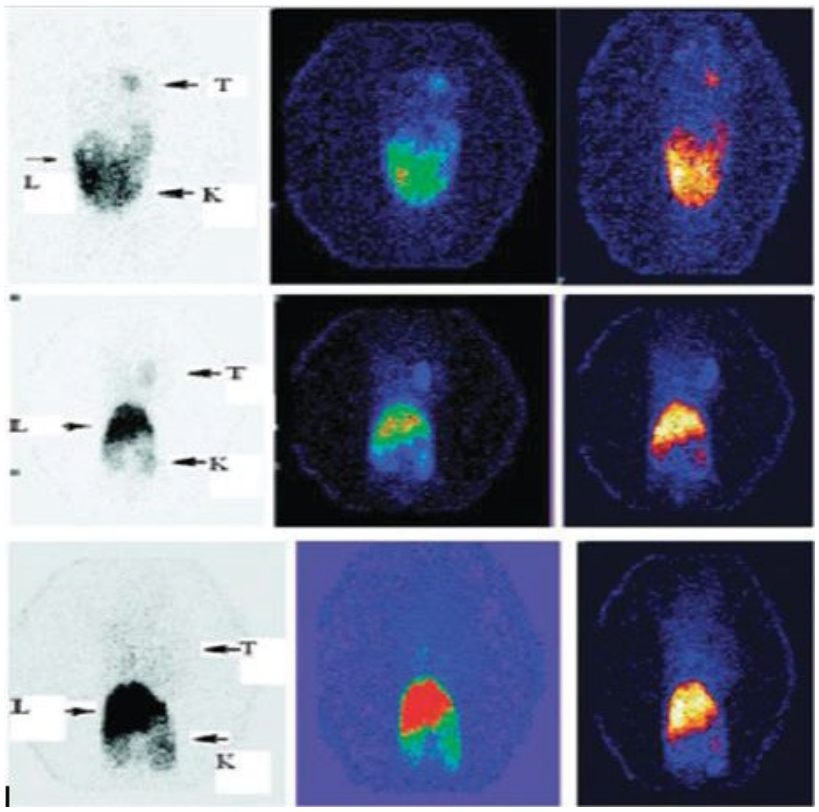

Figure 5: Micro-SPECT images of KB tumour-bearing nude mice at 4 h: T, tumour; L, lungs; K, kidney (upper images for technetium labelled G5 PAMAM-PEG-FA, middle images for technetium labelled G5 PAMAM-FA 2, and lower images for technetium labelled G5 PAMAM).

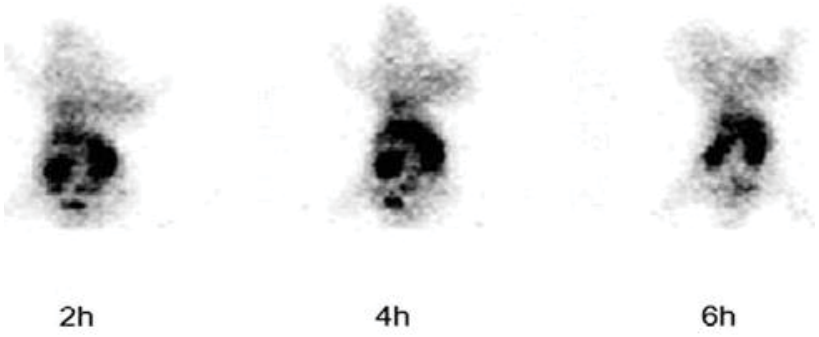

Figure 6: SPECT image of KB-bearing nude mice at 2, 4 and 6 h after injection the tracer.

Xu et al. also evaluated dendrimers as SPECT imaging agents. However the conjugate containing folic acid molecule has much accumulation in kidneys, so they tried to employ avid in instead of folic acid to observe the biodistribution and micro-SPECT imaging. They synthesized and characterized ^{99m}Tc radio-labeled acetylated dendrimer–avidin conjugates. The radio-labeled conjugate of Avidin-G5-Ac81-1B4M10-^{99m}Tc was successfully prepared and characterized which exhibits excellent *in vitro/in vivo* stability and rapid clearance from blood. The *in vitro* cell uptake assay revealed that the conjugate for Avidin-G5-Ac81-1B4M10-^{99m}Tc could bind efficiently to HeLa cell, both of the *in vivo* biodistribution and micro-SPECT imaging study shows that the high uptake was observed in liver and spleen while low in the kidney (Figure 4) [62]. In their study, after receiving the same dose of labeled compound Av-G5-Ac81-1B4M10-^{99m}Tc, animals were euthanized at the designated times and selected tissues were removed, weighed, and counted to determine ^{99m}Tc distribution. The percentages of ID/g in normal mice at 2 h, 4 h and 6 h post-injection of Av-G5-Ac81-1B4M10-^{99m}Tc were shown in Table 3.

In addition, acetylated PAMAM (G5-Ac) was conjugated with biotin and 2-(p-isothiocyanatobenzyl)-6-methyl-diethylenetria minepentaacetic acid (1B4M-DTPA), respectively to form the complex Bt-G5-Ac-1B4M which was further conjugated with avidin to give the conjugate Av-G5-Ac-1B4M. Both of the conjugates were radio-labeled with ^{99m}Tc, respectively. *In vitro* cellular uptake study showed that the conjugate of Av-G5-Ac-1B4M-^{99m}Tc exhibits much higher cellular uptake in HeLa cells than that of Bt-G5-Ac-1B4M-^{99m}Tc [63]. According to these researches about *in vitro/in vivo* stability, biodistribution and

micro-SPECT imaging was observed only for the conjugate of Av-G5-Ac-1B4M-^{99m}Tc. In another study, PAMAM dendrimers G4 were labeled with ^{99m}Tc and conjugated with Fluoresceinisothiocyanate (FITC) (Figure 7).

Moreover, dendrimers such as Eu-G3P4A18N, which are build of G3 PAMAM dendrimers may be used in imaging studies for detection of the distribution sites of metastatic hepatic colorectal tumors [64]. Fluorinated dendrimers may act as surfactants in biphasic systems (water/supercritical CO_2) or as phase transfer catalysts of anionic species from water to supercritical fluids [65,66]. Thanks to the large and well-defined surface area of a dendrimer, they are ideal agents for sensing ions and gases. Metallo-dendrimers are the second type of dendrimers that may be utilized as carriers for catalysts. Furthermore, these types of macromolecules are promising substrates for multielectroredox processes, photochemistry and photophysics [65]. Catalytic activity present also palladium-based dendrimer-encapsulated metal nanoparticles (DEMNs) [67] and Cu (II)-PAMAM dendrimers [68]. Photophysical properties exhibit also ionic liquid crystals based on PAMAM and PPI dendrimers (Table 4) [69].

As far a smulti-imaging, low-generation dendrimers, G2 maximum, can be used instead of their more complex, time consuming, and high generation contrary. Application of small size dendrimer is beneficial at all of aspects such as, synthetic accessibility, reproducibility and characterization, complete elimination from the body. Therefore, physical size of a dendrimer, which can be controlled by its generation, the charges and hydrophilicity affect the dendrimer's pharmacokinetics and pharmacodynamics. However, the application of dendrimers to nuclear medicine and radiochemistry is still in its infancy. But rapid technological and scientific progresses in bioimaging, nanomedicine and theragnosis, will provide new research opportunities for biodendrimer scientists in the preclinical and clinical development of new therapies [70].

Recently, Hamidi et al. synthesized aldehyde terminated dendrimers (Polyamidoaldehyde (PAMAL) dendrimers) using aminoacetaldehydedimethylacetal instead of glutaraldehyde and prevent side chain crosslinking problem in producing dendrimers with terminal aldehyde group, successfully. Their research shows that PAMAL has lower toxicity than PAMAM dendrimers in cell cultures (MCF7 breast cancer cell line), which can good choice for diagnostic and especial therapeutics procedures (Figure 8).

SPECT has continued to dominate due to lower cost and use of generator-based radionuclides as compared to PET, which required higher infrastructure cost of cyclotron and radiochemistry facilities. Therefore, better radiotracer design has to be combined with improvements in hardware to improve image quality [71,72].

Organs	2 h	4 h	6 h
Blood	1.44 ± 0.05 a	0.91 ± 0.21	0.77 ± 0.02
Heart	2.48 ± 022	238 ± 0.75	124 ± 0.01
Liver	45.55 ± 2.14	47.74 ± 1.33	56541 ± 130
Spleen	43.80 ± 0.50	4738 ± 2.00	51.09 ± 5.99
Lung	12.56 ± 3.02	9393 ± 1.81	731 ± 292
Kidney	2.121 ± 0.17	228 ± 0.01	335 ± 0.40
Intestine	0.84 ± 0.18	0.45 ± 0.15	0A4 ± 0.06
Stomach	022 ± 007	0.51 ± 0.01	0448 ± 0.05
Muscle	0.24 ± 0.01	0.18 ± 0.05	0.16 ± 0.02
Skin	0.69 ± 0.26	0.57 ± 0.12	051 ± 13.08
Bone	0.67 ± 0.02	0.553 ± 0.09	0447 ± 0.01
Brain	0.04 ± 0.01	0.04 ± 0.02	OAS ± 0.01
[a]Values are shown as mean ± SD (id/g)(n=3)			

Table 3: Bioditribution of Avidin-G5-AC81-1B4M10 ^{99m}TC 2, 4 and 6 h after injection the tracer in normal mice.

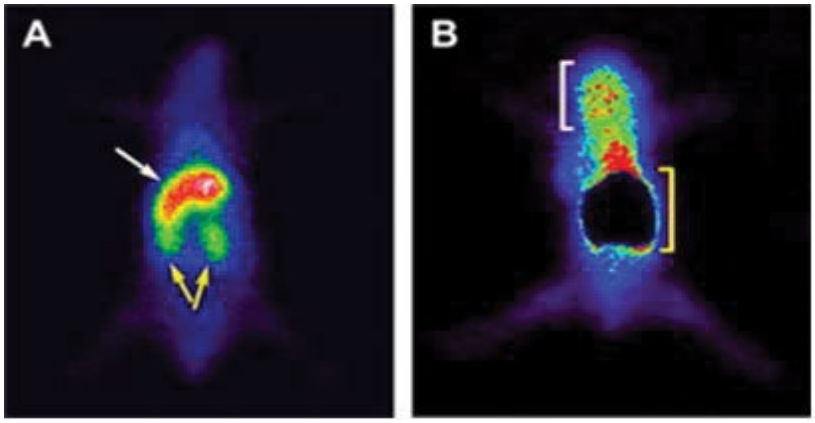

Figure 7: Scintigraphy image of normal (a) and melanoma-bearing mice (b) injected with ^{99m}Tc (CO)3-dendrimer-FITC, 1 h post-injection. (a) White and yellow arrows point liver and kidneys respectively. (b) White bracket shows the region where the tumor was located. Yellow bracket shows the abdominal region (liver and kidneys) where mask was placed in order to avoid image interference with tumor region. Low uptake observed in surrounding muscle tissues provides good contrast for tumor imaging.

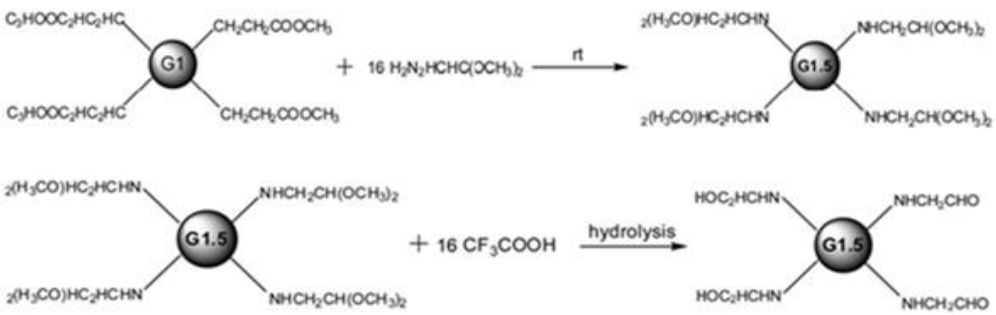

Figure 8: Synthesis pathway of aldehyde terminated dendrimers (G2).

Target	SPECT radiotracer/ligand
Regional cerebral perfusion	^{99m}Tc-bicisate (ECD, Neurolite), ^{99m}Tc-exametazime (HMPAO, Ceretec), [^{123}Idiodoamphetamine (^{123}SIJIMP)
Cerebrospinal fluid kinetics	^{111}In-Pentetate
Phosphatidylserine - dementia	^{99m}TC-HYNIC - annexin V
Dopamine D2, D3 receptors	[^{123}I] iodobenzamide (IBZM), [^{123}I epidepride]
Dopamine reuptake transporter	[^{123}I] ioflupane, [^{123}I] altropane, ^{99m}Tc-TRODAT
Peripheral benzodiazepine receptor (PBR)	[^{123}I] PK11195
Amyloid	[^{123}I] IMPY
Serotonin teuptake transporter (SERT)	[^{123}I] IDAM, [^{123}I] JADAM
GABA receptor	[^{123}I] diomazenil

Table 4: Common radiotracers for neurology assessments.

Conclusion

Conjugating radiopharmaceuticals and dendrimers has produced bioimaging probes which have prolonged enhanced stability, reduced toxicity and improved target specificity. However, the application of dendrimers to nuclear medicine is still new technique for improving images. Pharmaceuticals may be encapsulated in dendrimers, physically adsorbed or chemically attached on to the dendrimer surface. Therefore, since these nanoparticles conjugated with radio tracers like ^{99m}TC, quality of images in the region of interest increased. Overall, the multidisciplinary structure of dendrimers makes them good choices for medical imaging or treatment.

References

1. Hamoudeh M, Kamleh MA, Diab R, Fessi H (2008) Radionuclides delivery systems for nuclear imaging and radiotherapy of cancer. Adv Drug Deliv Rev 60: 1329-1346.
2. Miller TR (1996) The AAPM/RSNA physics tutorial for residents. Clinical aspects of emission tomography. RadioGraphics 16: 661-668.
3. Blankespoor SC, Xu X, Kaiki K, Brown JK, Tang HR, et al. (1996) Attenuation correction of SPECT using X-ray CT on an emission-transmission CT system: Myocardial perfusion assessment. Nucl Sci IEEE Trans On 43: 2263-2274.
4. Townsend DW, Beyer T, Blodgett TM (2003) PET/CT scanners: A hardware approach to image fusion. Seminars in nuclear medicine. Semin Nucl Med 33: 193-204.
5. Yeung HW, Schöder H, Smith A, Gonen M, Larson SM (2005) Clinical value of combined positron emission tomography/computed tomography imaging in the interpretation of 2-deoxy-2-[F-18] fluoro-d-glucose–positron emission tomography studies in cancer patients. Mol Imaging Biol 7: 229-235.
6. Park JH, Lee S, Kim JH, Park K, Kim K, et al. (2008) Polymeric nanomedicine for cancer therapy. Prog Polym Sci 33: 113-137.
7. Kopeček J, Kopečková P, Minko T, Lu ZR, Peterson CM (2001) Water soluble polymers in tumor targeted delivery. J Controlled Release 74: 1470-1158.
8. Jensen KD, Nori A, Tijerina M, Kopečková P, Kopeček J (2003) Cytoplasmic delivery and nuclear targeting of synthetic macromolecules. J Controlled Release 21: 89-105.
9. Matsumura Y, Maeda H (1986) A new concept for macromolecular therapeutics in cancer chemotherapy: Mechanism of tumoritropic accumulation of proteins and the antitumor agent smancs. Cancer Res 46: 6387-6392.
10. Maeda H, Seymour LW, Miyamoto Y (1992) Conjugates of anticancer agents and polymers: Advantages of macromolecular therapeutics in vivo. Bioconjug Chem 3: 351-362.
11. Maeda H, Wu J, Sawa T, Matsumura Y, Hori K (2000) Tumor vascular permeability and the EPR effect in macromolecular therapeutics: A review. J Controlled Release 65: 271-284.
12. Khandare J, Minko T (2006) Polymer-drug conjugates: Progress in polymeric prodrugs. Prog Polym Sci 31: 359-397.
13. Lu ZR, Shiah JG, Sakuma S, Kopečková P, Kopeček J (2002) Design of novel bioconjugates for targeted drug delivery. J Controlled Release 78: 165-173.
14. Fréchet JM (2003) Dendrimers and other dendritic macromolecules: From building blocks to functional assemblies in nanoscience and nanotechnology. J Polym Sci Part Polym Chem 41: 3713-3725.
15. Tomalia DA (2005) Birth of a new macromolecular architecture: Dendrimers as quantized building blocks for nanoscale synthetic polymer chemistry. Prog Polym Sci 30: 294-324.
16. Ryding E (1996) SPECT measurements of brain function in dementia; a review. Acta Neurol Scand 94: 54-58.
17. Pimlott SL, Ebmeier KP (2007) SPECT imaging in dementia. Br J Radiol 2: 153-159.
18. Valotassiou V, Wozniak G, Sifakis N, Demakopoulos N, Georgoulias P (2008) Radiopharmaceuticals in neurological and psychiatric disorders. Curr Clin Pharmacol 3: 99-107.
19. Kung MP, Zhuang ZP, Hou C, Kung HF (2004) Development and evaluation of iodinated tracers targeting amyloid plaques for SPECT imaging. J Mol Neurosci 24: 49-53.
20. Agdeppa ED, Spilker ME (2009) A review of imaging agent development. AAPS J 11: 286-99.
21. Slomka PJ, Patton JA, Berman DS, Germano G (2009) Advances in technical aspects of myocardial perfusion SPECT imaging. J Nucl Cardiol 16: 255-276.

22. Bybel B, Brunken RC, DiFilippo FP, Neumann DR, Wu G (2008) SPECT/CT imaging: clinical utility of an emerging technology. Radiogr Rev Publ Radiol Soc N Am Inc 28: 1097-1113.

23. Zaidi H, Koral KF (2004) Scatter modelling and compensation in emission tomography. Eur J Nucl Med Mol Imaging 31: 761-82.

24. Jansen FP, Vanderheyden JL (2007) The future of SPECT in a time of PET. Nucl Med Biol 34: 733-735.

25. Uematsu T, Yuen S, Yukisawa S, Aramaki T, Morimoto N, et al. (2005) Comparison of FDG PET and SPECT for detection of bone metastases in breast cancer. Am J Roentgenol 184: 1266-1273.

26. Herholz K, Schopphoff H, Schmidt M, Mielke R, Eschner W, et al. (2002) Direct comparison of spatially normalized PET and SPECT scans in Alzheimer's disease. J Nucl Med 43: 21-26.

27. Richards P (1960) A survey of the production at Brookhaven National Lab of the isotopes for medical research. Trans 5th Nuclear Congress, 7th Int Electronic and Nuclear Symp p. 225.

28. Rayudu GS (1983) Radiotracers for medical applications. CRC Press Inc Boca.

29. Deutsch E, Libson K, Jurisson S, Lindoy LF (1983) Technetium chemistry and technetium radiopharmaceuticals. Prog Inorg Chem 30: 139.

30. Nunn AD, Loberg MD, Conley RA (1983) A structure-distribution-relationship approach leading to the development of Tc-99m mebrofenin: An improved cholescintigraphic agent. J Nucl Med Off Publ Soc Nucl Med 24: 423-430.

31. Banerjee S, Pillai MRA, Ramamoorthy N (2001) Evolution of Tc-99m in diagnostic radiopharmaceuticals. Semin Nucl Med 31: 260-277.

32. Gabriel M, Decristoforo C, Donnemiller E, Ulmer H, Rychlinski CW, et al. (2003) An intrapatient comparison of 99mTc-EDDA/HYNIC-TOC with 111In-DTPA-octreotide for diagnosis of somatostatin receptor-expressing tumors. J Nucl Med 44: 708-716.

33. Riccabona G, Decristoforo C (2003) Peptide targeted imaging of cancer. Cancer Biother Radiopharm 18: 675-687.

34. Caminade AM, Turrin CO, Majoral JP (2010) Biological properties of phosphorus dendrimers. New J Chem 34: 1512-1524.

35. Tomalia DA, Baker H, Dewald J, Hall M, Kallos G, et al. (1985) A new class of polymers: Starburst-dendritic macromolecules. Polym J 17: 117-32.

36. Subbarayan M, Shetty SJ, Srivastava TS, Noronha OP, Samuel AM, et al. (2001) Water-soluble 99mTc-labeled dendritic novel porphyrins tumor imaging and diagnosis. Biochem Biophys Res Commun 16: 32-36.

37. Agashe HB, Babbar AK, Jain S, Sharma RK, Mishra AK, et al. (2007) Investigations on biodistribution of technetium-99m-labeled carbohydrate-coated poly (propylene imine) dendrimers. Nanomedicine Nanotechnol Biol Med 3: 120-127.

38. Hecht S, Fréchet JM (2001) Dendritic encapsulation of function: Applying nature's site isolation principle from biomimetics to materials science. Angew Chem Int Ed 40: 74-91.

39. Zhang Y, Sun Y, Xu X, Zhang X, Zhu H, et al. (2010) Synthesis, biodistribution, and microsingle photon emission computed tomography (spect) imaging study of technetium-99m labeled pegylated dendrimer poly (amidoamine)(pamam)-folic acid conjugates. J Med Chem 53: 3262-3272.

40. Salazar MD, Ratnam M (2007) The folate receptor: What does it promise in tissue-targeted therapeutics? Cancer Metastasis Rev 26: 141-152.

41. Zhang Y, Sun Y, Xu X, Zhang X, Zhu H, et al. (2010) Synthesis, Biodistribution, and Microsingle Photon Emission Computed Tomography (SPECT) Imaging Study of Technetium-99m Labeled PEGylated Dendrimer Poly (amidoamine) (PAMAM)- Folic Acid Conjugates. J Med Chem 53: 32682-3292.

42. Shukla R, Thomas TP, Peters JL, Desai AM, Kukowska-Latallo J, et al. (2006) HER2 specific tumor targeting with dendrimer conjugated anti-HER2 mAb. Bioconjug Chem 17: 1109-1115.

43. Salazar MD, Ratnam M (2007) The folate receptor: What does it promise in tissue-targeted therapeutics? Cancer Metastasis Rev 26: 141-152.

44. Low PS, Henne WA, Doorneweerd DD (2007) Discovery and development of folic-acid-based receptor targeting for imaging and therapy of cancer and inflammatory diseases. Acc Chem Res 41: 120-129.

45. Low PS, Antony AC (2004) Folate receptor-targeted drugs for cancer and inflammatory diseases. Adv Drug Deliv Rev 56: 1055-1058.

46. Patri AK, Kukowska Latallo JF, Baker JR (2005) Targeted drug delivery with dendrimers: Comparison of the release kinetics of covalently conjugated drug and non-covalent drug inclusion complex. Adv Drug Deliv Rev 57: 2203-2214.

47. Majoros IJ, Thomas TP, Mehta CB, Baker JR (2005) Poly (amidoamine) dendrimer-based multifunctional engineered nanodevice for cancer therapy. J Med Chem 48: 5892-5899.

48. Myc A, Majoros IJ, Thomas TP, Baker JR (2007) Dendrimer-based targeted delivery of an apoptotic sensor in cancer cells. Biomacromolecules 8: 13-18.

49. Thomas TP, Majoros IJ, Kotlyar A, Kukowska-Latallo JF, Bielinska A, et al (2005) Targeting and inhibition of cell growth by an engineered dendritic nanodevice. J Med Chem 48: 3729-3735.

50. Yang W, Cheng Y, Xu T, Wang X, Wen L (2009) Targeting cancer cells with biotin-dendrimer conjugates. Eur J Med Chem 44: 862-868.

51. Hill E, Shukla R, Park SS, Baker Jr JR (2007) Synthetic PAMAM–RGD conjugates target and bind to odontoblast-like MDPC 23 cells and the predentin in tooth organ cultures. Bioconjug Chem 18: 1756-1762.

52. Lesniak WG, Kariapper MS, Nair BM, Tan W, Hutson A, et al. (2007) Synthesis and characterization of PAMAM dendrimer-based multifunctional nanodevices for targeting αvβ3 integrins. Bioconjug Chem 18: 1148-1154.

53. Shi X, Wang S, Meshinchi S, Van Antwerp ME, Bi X, et al. (2007) Dendrimer-entrapped gold nanoparticles as a platform for cancer-cell targeting and imaging. Small 3: 1245-1252.

54. Shi X, Majoros IJ, Patri AK, Bi X, Islam MT, et al. (2006) Molecular heterogeneity analysis of poly (amidoamine) dendrimer-based mono-and multifunctional nanodevices by capillary electrophoresis. Analyst 131: 374-381.

55. Zhang Y, Sun Y, Xu X, Zhu H, Huang L, et al. (2010) Radiosynthesis and micro-SPECT imaging of 99m Tc-dendrimer poly (amido)-amine folic acid conjugate. Bioorg Med Chem Lett 20: 927-931.

56. Parrott MC, Benhabbour SR, Saab C, Lemon JA, Parker S, et al. (2009) Synthesis, radiolabeling, and bio-imaging of high-generation polyester dendrimers. J Am Chem Soc 131: 2906-2916.

57. Mamede M, Saga T, Ishimori T, Higashi T, Sato N, et al. (2004) Hepatocyte targeting of 111In-labeled oligo-DNA with avidin or avidin–dendrimer complex. J Controlled Release 20: 133-141.

58. Yao Z, Zhang M, Sakahara H, Saga T, Arano Y, et al. (1998) Avidin targeting of intraperitoneal tumor xenografts. J Natl Cancer Inst 7: 25-29.

59. Yao Z, Zhang M, Sakahara H, Saga T, Nakamoto Y, et al. (1998) Imaging of intraperitoneal tumors with technetium-99m GSA. Ann Nucl Med 12: 115-118.

60. Yao Z, Zhang M, Sakahara H, Nakamoto Y, Higashi T, et al. (1999) The relationship of glycosylation and isoelectric point with tumor accumulation of avidin. J Nucl Med Off Publ Soc Nucl Med 40: 479-483.

61. Kobayashi H, Sakahara H, Hosono M, Yao ZS, Toyama S, et al. (1994) Improved clearance of radiolabeled biotinylated monoclonal antibody following the infusion of avidin as a "chase" without decreased accumulation in the target tumor. J Nucl Med Off Publ Soc Nucl Med 35: 1677-1684.

62. Xu X, Zhang Y, Wang X, Guo X, Zhang X, et al. (2011) Radiosynthesis, biodistribution and micro-SPECT imaging study of dendrimer–avidin conjugate. Bioorg Med Chem 19: 1643-1648.

63. Tassano MR, Audicio PF, Gambini JP, Fernandez M, Damian JP, et al. (2011) Development of 99m Tc (CO) 3-dendrimer-FITC for cancer imaging. Bioorg Med Chem Lett 21: 5598-5601.

64. Alcala MA, Kwan SY, Shade CM, Lang M, Uh H, et al. (2011) Luminescence targeting and imaging using a nanoscale generation 3 dendrimer in an in vivo colorectal metastatic rat model. Nanomedicine Nanotechnol Biol Med 7: 249-258.

65. Caminade AM, Turrin CO, Sutra P, Majoral JP (2003) Fluorinated dendrimers. Curr Opin Colloid Interface Sci 8: 282-295.

66. Brauge L, Veriot G, Franc G, Deloncle R, Caminade AM, et al. (2006) Synthesis of phosphorus dendrimers bearing chromophoric end groups: toward organic blue light-emitting diodes. Tetrahedron 62: 11891-11899.

67. Sato N, Kobayashi H, Saga T, Nakamoto Y, Ishimori T, et al. (2001) Tumor targeting and imaging of intraperitoneal tumors by use of antisense oligo-DNA complexed with dendrimers and/or avidin in mice. Clin Cancer Res 7: 3606-3612.

68. Jarzębińska A, Pietraszkiewicz M, Bilewicz R (2001) Nanoscopic complexes of dendrimers based on hexaazamacrocycle—synthesis and characterization. Mater Sci Eng C 1: 61-64.

69. Gu C, Xiong K, Shentu B, Zhang W, Weng Z (2010) Catalytic Cu (II)- amine terminated poly (amidoamine) dendrimer complexes for aerobic oxidative polymerization to form poly (2, 6-dimethyl-1, 4-phenylene oxide) in water. Macromolecules 43: 1695-1698.

70. Ghobril C, Lamanna G, Kueny SM, Garofalo A, Billotey C, et al. (2012) Dendrimers in nuclear medical imaging. New J Chem 36: 310-323.

71. Hamidi A, Rashidi MR, Asgari D, Aghanejad A, Davaran S (2012) Covalent Immobilization of Trypsin on a Novel Aldehyde-Terminated PAMAM Dendrimer. Bull Korean Chem Soc 33: 2181-2186.

72. Valliant JF (2010) A bridge not too far: Linking disciplines through molecular imaging probes. J Nucl Med 51: 1258-1268.